



Published in final edited form as:

Nat Med. 2013 April ; 19(4): 418–420. doi:10.1038/nm.3104.

Human PXR modulates hepatotoxicity associated with rifampicin and isoniazid co–therapy

Feng Li¹, Jie Lu¹, Jie Cheng², Laiyou Wang^{1,3}, Tsutomu Matsubara², Iván L. Csanaky¹, Curtis D. Klaassen¹, Frank J. Gonzalez², and Xiaochao Ma¹

¹Department of Pharmacology, Toxicology and Therapeutics, the University of Kansas Medical Center, Kansas City, Kansas. ²Laboratory of Metabolism, Center for Cancer Research, National Cancer Institute, National Institutes of Health, Bethesda, Maryland.

Abstract

Rifampicin and isoniazid co–therapy frequently causes liver injury in humans. A pregnane X receptor–humanized mouse model revealed that rifampicin and isoniazid co–treatment causes accumulation of protoporphyrin IX, an endogenous hepatotoxin, in the liver via a pregnane X receptor–mediated alteration of heme biosynthesis pathway. These results provide novel insight into the mechanism of rifampicin and isoniazid–induced liver injury that may be applied to clinical management of the hepatotoxicity associated with tuberculosis chemotherapy.

Tuberculosis (TB) is a global health problem and chemotherapy is the most effective method of TB control. A major issue during TB treatment is drug–induced liver injury ¹. Once liver injury occurs, the anti–TB regimen has to be altered or discontinued, which can result in TB relapse, drug resistance, and TB–related death. Both rifampicin (RIF) and isoniazid (INH) are first–line anti–TB drugs. The combination of these two drugs is highly effective. However, this combination frequently causes liver injury, and even liver failure. Extensive studies were conducted to investigate liver injury caused by RIF and INH in mice and rats ^{2–4}; nevertheless, these studies poorly mimicked the hepatotoxicity in humans. Species differences between rodents and humans in responding to RIF or INH are expected.

Pregnane X receptor (PXR) is a ligand–dependent transcription factor regulating a gene network involved in metabolism of xenobiotics and endobiotics ⁵. The ability of chemicals to activate PXR is species–dependent. RIF is a human PXR–specific activator that has a very weak effect on mouse PXR ⁶. To overcome the species differences in RIF–mediated PXR activation, *PXR*–humanized (hPXR) mice were used in the current study. In hPXR

Users may view, print, copy, download and text and data–mine the content in such documents, for the purposes of academic research, subject always to the full Conditions of use: http://www.nature.com/authors/editorial_policies/license.html#terms

Correspondence should be addressed to X.M. (xma2@kumc.edu).

³Current affiliation: Department of Pharmacology, Guangdong Pharmaceutical University, Guangzhou, China.

AUTHOR CONTRIBUTIONS

F.L., J.L., J.C., L.W., T.M., I.L.C. and X.M. performed the experiments. C.D.K. and F.J.G. contributed to the scientific discussion and manuscript editing. X.M. and F.L. conceived the project and wrote the manuscript.

COMPETING FINANCIAL INTERESTS

The authors declare no competing financial interests.

mice co-treated with RIF and INH (Supplementary Fig. 1), significant increases in serum alanine aminotransferase (ALT) and alkaline phosphatase (ALP) activity were noted, but not in wild-type (WT) or *Pxr*-null mice (Fig. 1a–d). Bile plugs in liver were observed in hPXR mice co-treated with RIF and INH (Fig. 1e, Supplementary Fig. 2), which averaged 2.38 per view of liver sections at 100X magnification. This phenotype was not observed in WT (Fig. 1f) or *Pxr*-null (Fig. 1g) mice under the same treatment, or in the other hPXR groups (control, RIF or INH) (Fig. 1h–j). These results indicate that human PXR is a key modulator of the hepatotoxicity produced by RIF and INH co-therapy. Notably, these phenotypes mimic the hepatotoxicity in TB patients under RIF and INH chemotherapy. In a clinical trial of RIF and INH co-therapy, bile pigments were observed in 17 of 28 subjects (60.7%) as revealed by liver biopsies, and the elevation of ALT activity was in accordance with the degree of pathological changes⁷. The current studies show bile plugs in a mouse model for the first time and suggest that the hPXR mouse model is an appropriate model to study the liver injury produced by RIF and INH co-treatment.

The risk of hepatotoxicity is considerably higher in patients who are receiving both RIF and INH than RIF or INH alone⁸. INH hepatotoxicity is thought to be dependent upon metabolic activation by arylamine *N*-acetyltransferase and CYP2E1^{9,10}. RIF is a potent enzyme inducer in humans, so it was proposed that RIF potentiates INH hepatotoxicity *via* enzymatic induction and subsequent metabolic activation of INH¹¹. However, RIF does not regulate arylamine *N*-acetyltransferase or CYP2E1 expression^{12,13}. Acetylhydrazine (AcHZ) and hydrazine (HZ) are INH metabolites that were proposed to be responsible for INH-induced liver injury^{14,15}. In the current study, INH, AcHZ and HZ were individually administered to hPXR mice together with RIF. Liver injury was only observed in hPXR mice co-treated with RIF and INH (Supplementary Fig. 3), suggesting that AcHZ and HZ do not cause INH-related hepatotoxicity. In a recent report, a reactive metabolite of INH itself was identified¹⁶. However, RIF pretreatment does not potentiate INH bioactivation (Supplementary Fig. 4). Thus, a novel mechanism independent of INH metabolism is expected for the liver injury associated with RIF and INH co-therapy.

The bile metabolomes in hPXR mice were investigated to provide mechanistic clues to RIF and INH-induced hepatotoxicity. Metabolomic analysis revealed two clusters corresponding to the control and the RIF and INH co-treated groups (Fig. 2a), suggesting substantial differences in the chemical components between these two groups. The corresponding *S*-plot displays the ion contribution to this group separation (Fig. 2b). The highest ranking ion was not RIF or its metabolite, but an endogenous chemical, protoporphyrin IX (PPIX) (Fig. 2b). The identity of PPIX was confirmed by comparing it with an authentic standard (Supplementary Fig. 5). Extremely high concentrations of PPIX in bile were noted in hPXR mice co-treated with RIF and INH, but not in the other hPXR groups (control, RIF or INH) (Fig. 2c). PPIX is an intermediate in porphyrin biosynthesis. Normally, the concentrations of porphyrin intermediates, including PPIX, are very low in the liver. However, mutations of the ferrochelatase gene cause erythropoietic protoporphyria, a disease of porphyrin metabolism characterized by abnormally elevated levels of PPIX in blood and liver. High concentrations of PPIX in liver are known to cause liver injury^{17,18}. In the current study, high concentrations of PPIX in bile were noted in hPXR mice co-treated with RIF and INH,

but not in WT or *Pxr*-null mice under the same treatment (Fig. 2d). These data provide a link between PPIX and the PXR-mediated liver injury caused by RIF and INH co-therapy.

Aminolevulinic acid synthase (ALAS) is the rate limiting enzyme in porphyrin biosynthesis. Activation of PXR is known to up-regulate ALAS1 expression in liver¹⁹. Because PXR is predominantly expressed in the liver^{5,6}, PXR activation has no or very weak effect on ALAS expression in other organs, including bone marrow. Aminolevulinic acid (ALA) is the product of ALAS1 and it is a precursor of PPIX. In hPXR mice co-treated with ALA, RIF and INH, more significant liver injury was noted when compared to RIF and INH co-treated group (Fig. 2e and 2f). These data illustrate that RIF and INH co-therapy targets porphyrin biosynthesis and results in hepatic PPIX accumulation and liver injury. These results also explain why RIF and INH are contraindicated in patients with porphoria²⁰. In summary, this study offers a new paradigm for understanding the mechanism of liver injury associated with RIF and INH co-therapy. Novel strategies, based upon human PXR, ALAS, and PPIX, are expected to predict, prevent, and treat RIF and INH-induced liver injury.

METHODS

Animals and reagents

WT, *Pxr*-null, and hPXR mice (2–4 months old, male) were used in the current study. hPXR mice were generated by bacterial artificial chromosome transgenesis in *Pxr*-null mice^{21,22}. All mice were maintained under a standard 12-h dark and 12-h light cycle with water and chow provided ad libitum. Handling was in accordance with study protocols approved by the National Cancer Institute and the University of Kansas Medical Center Institutional Animal Care and Use Committee. Rifampicin (RIF), isoniazid (INH), hydrazine (HZ), acetylhydrazine (AChZ), aminolevulinic acid (ALA), and *N*- α -acetyl-L-lysine (NAL) were purchased from Sigma-Aldrich. All solvents for liquid chromatography and mass spectrometry were of the highest grade commercially available.

Experimental Design

Role of human PXR in liver injury caused by RIF and INH co-treatment—WT, *Pxr*-null, and hPXR mice were treated with INH, RIF, or RIF plus INH. INH was dissolved in drinking water (400 mg L⁻¹). RIF was added in diet (100 mg kg⁻¹) and was provided by Dyets Inc. Four weeks after the treatment, blood and liver samples were collected for evaluation of liver injury. Blood concentrations of RIF and INH were analyzed by ultra-performance liquid chromatography coupled with quadrupole time-of-flight mass spectrometer (UPLC-QTOFMS).

Comparison of liver injury caused by the co-treatment of RIF and INH or RIF and INH metabolites—All the hPXR mice were fed a RIF-containing diet (100 mg kg⁻¹) and INH (400 mg L⁻¹, 2.9 mmol L⁻¹), or AChZ (200 mg L⁻¹, 2.7 mmol L⁻¹), or HZ (200 mg L⁻¹, 6.3 mmol L⁻¹)—containing water. Four weeks after treatment, blood and liver samples were collected for evaluation of liver injury. Concentrations of INH, AChZ and HZ in the liver were analyzed by UPLC-QTOFMS. Among these three groups, the highest

concentration of AcHZ in the liver was noted in AcHZ treated group, and the highest concentration of HZ in the liver was noted in HZ treated group (data not shown).

Effect of RIF on INH bioactivation—Mouse liver microsomes were prepared from hPXR mice, which were fed a control diet or a RIF-containing diet (100 mg kg⁻¹) for seven days. PXR activation was evaluated by monitoring hydroxylation of midazolam, a substrate of CYP3A. NAL was used to trap INH bioactivation²³.

Bile collection and metabolomic analysis—WT, *Pxr*-null, and hPXR mice were treated with INH, RIF, or RIF plus INH. INH was dissolved in drinking water (400 mg L⁻¹). RIF was added in diet (100 mg kg⁻¹). Four weeks after treatment, bile samples were collected from cannulated common bile ducts and analyzed by UPLC-QTOFMS in a positive mode. Bile metabolomes were generated by using MassLynx and MarkerLynx software (Waters) based on accurate mass measurement.

Effect of PPIX precursor on liver injury induced by RIF and INH co-treatment in hPXR mice—ALA is the product of ALAS1 and it is a precursor of PPIX. hPXR mice were fed a control diet and water (control), or a RIF-containing diet (100 mg kg⁻¹) and INH-containing water (400 mg L⁻¹) for two weeks. On the 15th day, ALA (100 mg kg⁻¹, ip, twice daily) was added to control or RIF and INH co-treated group for four more days. On the 20th day, all mice were killed to collect liver and blood samples for evaluation of liver injury.

Evaluation of liver injury—Serum biochemical and liver histological analysis were conducted to evaluate liver injury. Serum ALT and ALP activity were analyzed according to standard assay kit procedures. Liver specimens were fixed in 4% formaldehyde phosphate buffer. Liver sections were stained with hematoxylin and eosin.

UPLC-QTOFMS analysis—A 100 mm × 2.1 mm (Acquity 1.7 μm) UPLC BEH C-18 column (Waters) was used for metabolite separation. The flow rate of the mobile phase was 0.3 ml min⁻¹ with a gradient ranging from 2% to 98% aqueous acetonitrile containing 0.1% formic acid in a 10-min run. QTOFMS was operated in a positive mode with electrospray ionization. The source temperature and desolvation temperature were set at 120 °C and 350 °C, respectively. Nitrogen was applied as the cone gas (10 L h⁻¹) and desolvation gas (700 L h⁻¹). Argon was applied as collision gas. QTOFMS was calibrated with sodium formate and monitored by the intermittent injection of lock mass leucine enkephalin in real time. The capillary voltage and cone voltage were set at 3.5 kV and 35 V. Tandem mass spectrometry fragmentation was conducted with collision energy ramp ranging from 10 to 35 V.

Data analysis—Mass chromatograms and mass spectra were acquired by MassLynx software in centroid format from *m/z* 50 to *m/z* 1000. Centroid and integrated mass chromatographic data were processed by MarkerLynx software to generate a multivariate data matrix. The corresponding data matrices were then exported into SIMCA-P+12 (Umetrics) for multivariate data analysis. Orthogonal projection to latent structures-discriminant analysis was conducted on Pareto-scaled data. Screening and identification of major metabolites were performed by using MetaboLynx and MarkerLynx software based on

accurate mass measurement (mass errors <10 ppm). All quantified data are expressed as mean \pm S.E.M. Statistical differences between two groups were determined by Student's *t*-test.

Supplementary Material

Refer to Web version on PubMed Central for supplementary material.

ACKNOWLEDGMENTS

This work was supported by the National Institute of Diabetes and Digestive and Kidney Diseases [Grant number DK090305] and the National Cancer Institute Intramural Research Program. We thank Dr. Martha Montello for editing the manuscript.

REFERENCES

1. Saukkonen JJ, et al. *Am J Respir Crit Care Med*. 2006; 174:935–952. [PubMed: 17021358]
2. Yew WW, Leung CC. *Respirology*. 2006; 11:699–707. [PubMed: 17052297]
3. Chowdhury A, et al. *J Hepatol*. 2006; 45:117–126. [PubMed: 16545483]
4. Tasduq SA, Kaiser P, Sharma SC, Johri RK. *Hepatol Res*. 2007; 37:845–853. [PubMed: 17573957]
5. Kliewer SA, et al. *Cell*. 1998; 92:73–82. [PubMed: 9489701]
6. Lehmann JM, et al. *J Clin Invest*. 1998; 102:1016–1023. [PubMed: 9727070]
7. Xing T, Chen J, Zhang G. *Zhonghua Jie He He Hu Xi Za Zhi*. 1997; 20:33–35. [PubMed: 10072800]
8. Gangadharam PR. *Am Rev Respir Dis*. 1986; 133:963–965. [PubMed: 3013057]
9. Huang YS, et al. *Hepatology*. 2003; 37:924–930. [PubMed: 12668988]
10. Ohno M, et al. *Int J Tuberc Lung Dis*. 2000; 4:256–261. [PubMed: 10751073]
11. Miguet JP, Mavier P, Soussy CJ, Dhumeaux D. *Gastroenterology*. 1977; 72:924–926. [PubMed: 849823]
12. Slatter JG, et al. *Xenobiotica*. 2006; 36:938–962. [PubMed: 17118915]
13. Rosenfeld JM, Vargas R Jr, Xie W, Evans RM. *Mol Endocrinol*. 2003; 17:1268–1282. [PubMed: 12663745]
14. Mitchell JR, et al. *Annals of internal medicine*. 1976; 84:181–192. [PubMed: 766682]
15. Sarich TC, et al. *Archives of toxicology*. 1996; 70:835–840. [PubMed: 8911642]
16. Metushi IG, Nakagawa T, Uetrecht J. *Chemical research in toxicology*. 2012; 25:2567–2576. [PubMed: 23016703]
17. Casanova-Gonzalez MJ, Trapero-Marugan M, Jones EA, Moreno-Otero R. *World J Gastroenterol*. 2010; 16:4526–4531. [PubMed: 20857522]
18. Anstey AV, Hift RJ. *Gut*. 2007; 56:1009–1018. [PubMed: 17360790]
19. Fraser DJ, Zumsteg A, Meyer UA. *J Biol Chem*. 2003; 278:39392–39401. [PubMed: 12881517]
20. 2012. <http://www.porphyrria.uct.ac.za/professional/prof-tuberculosis.htm>

References for methods

21. Ma X, et al. *Drug Metab Dispos*. 2007; 35:194–200. [PubMed: 17093002]
22. Staudinger JL, et al. *Proc Natl Acad Sci U S A*. 2001; 98:3369–3374. [PubMed: 11248085]
23. Metushi IG, Nakagawa T, Uetrecht J. *Chemical research in toxicology*. 2012; 25:2567–2576. [PubMed: 23016703]

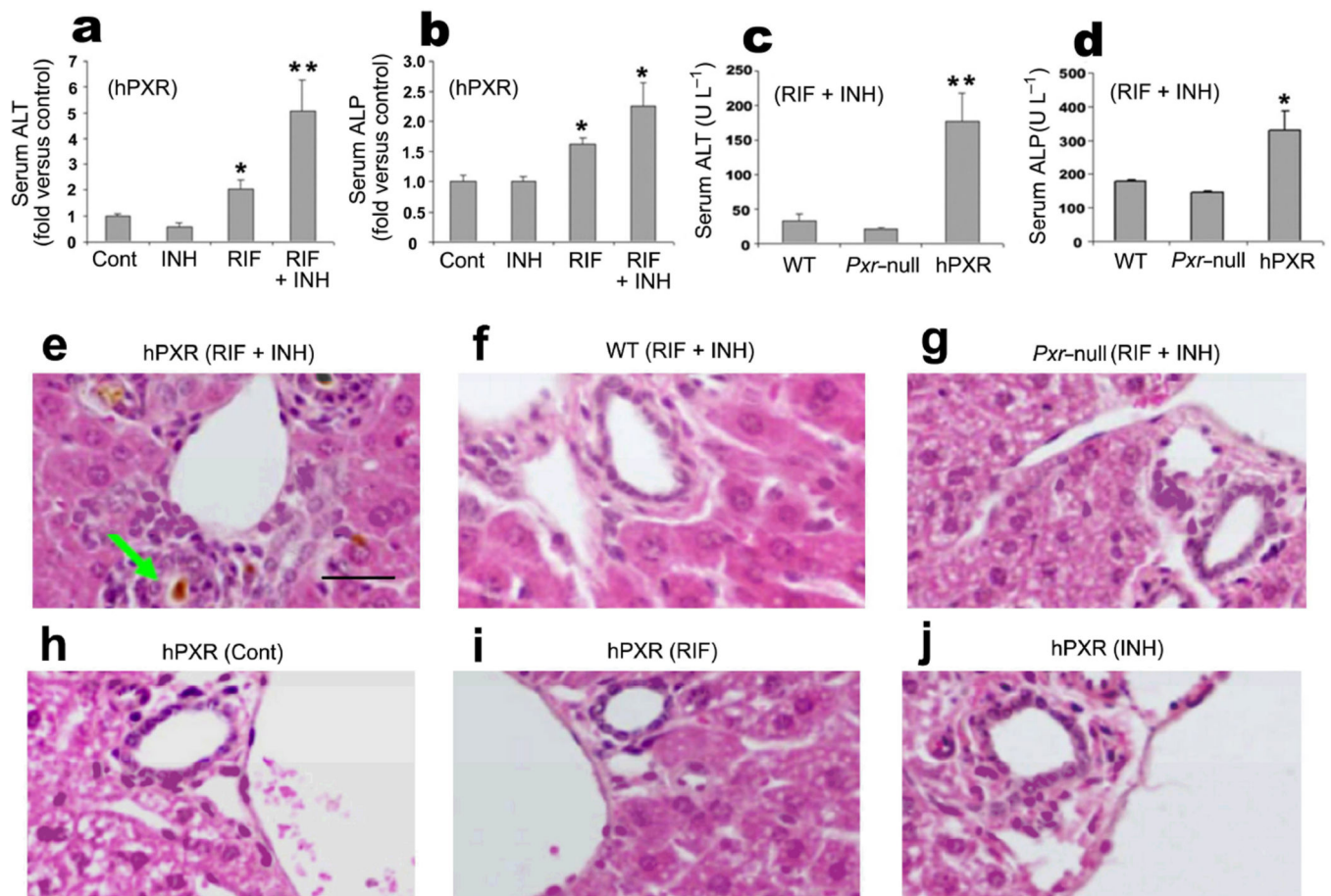


Figure 1. Hepatotoxicity associated with RIF and INH co-treatment is human PXR dependent WT ($n = 7$), *Pxr*-null ($n = 4$), and hPXR ($n = 4-9$) mice were treated with INH, RIF or RIF + INH. Blood and liver samples were collected after four weeks of treatment. (**a-d**) Biochemical analysis of serum ALT and ALP activity. The data are expressed as mean \pm S.E.M. ($n = 4$ in control and INH groups, $n = 7$ in RIF group, and $n = 9$ in RIF + INH group of hPXR mice). * $P < 0.05$ and ** $P < 0.01$ compared with the control group of hPXR mice (**a, b**), or WT mice (**c, d**). (**e-j**) Representative liver sections stained with hematoxylin and eosin. A bile plug is pointed by an arrow. Scale bar, 20 μ m.

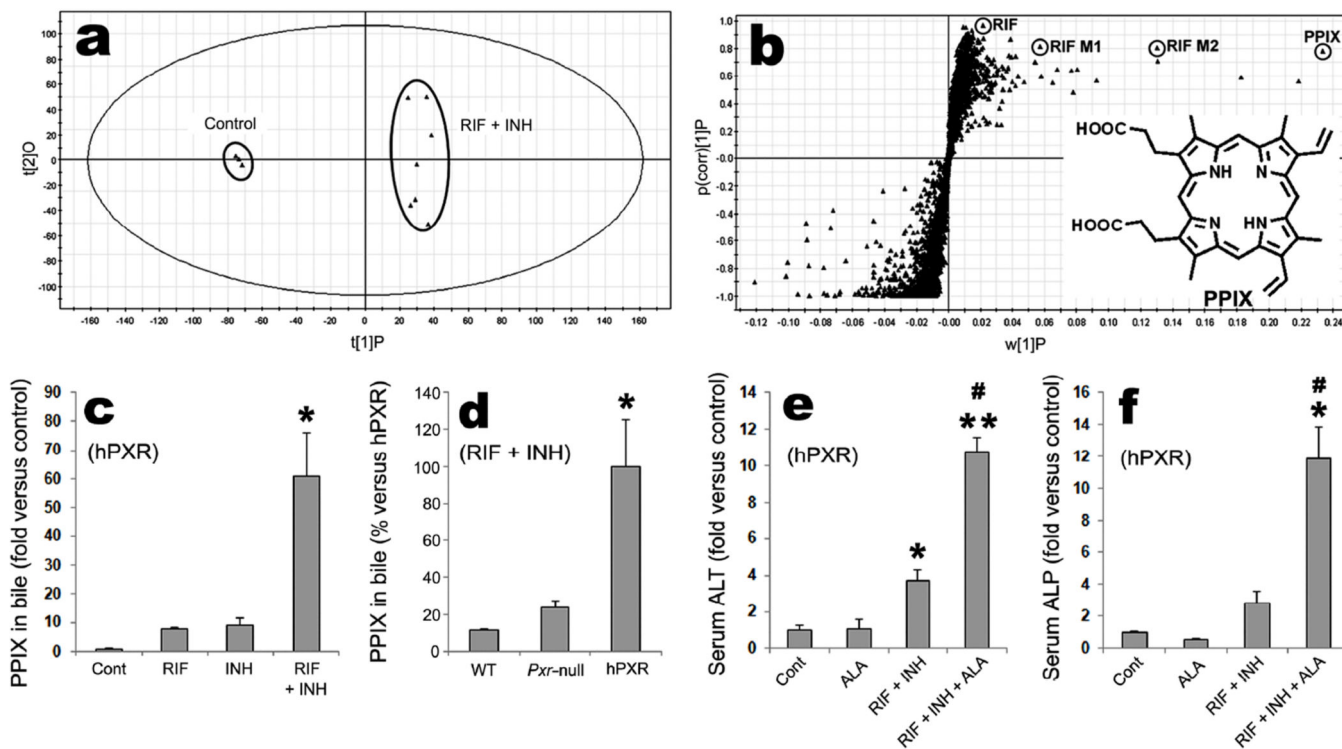


Figure 2. PPIX accumulation and the liver injury associated with RIF and INH co-therapy (a–d) Metabolomic analysis of bile and relative quantification of PPIX. (a) Separation of control and RIF and INH co-treated hPXR mouse bile in a score plot. (b) Loading *S*-plot generated by orthogonal projection to latent structures–discriminant analysis. Several top ranking ions were labeled, including RIF, RIF metabolites (M1 and M2), and PPIX. (c) Relative quantification of PPIX in bile of hPXR mice treated with vehicle ($n = 3$), RIF ($n = 3$), INH ($n = 5$), or RIF + INH ($n = 7$). PPIX concentration in the control group was set as 1. The data are expressed as mean \pm S.E.M. * $P < 0.05$ versus all other groups. (d) Relative quantification of PPIX in bile of WT ($n = 4$), *Pxr*-null ($n = 3$) and hPXR ($n = 7$) mice co-treated with RIF and INH. PPIX concentration in hPXR group was set as 100. The data are expressed as mean \pm S.E.M. * $P < 0.05$ versus WT or *Pxr*-null groups. (e, f) Effect of PPIX precursor on hepatotoxicity induced by RIF and INH co-treatment. Serum ALT (e) and ALP (f) activity were analyzed. The data are expressed as mean \pm S.E.M. ($n = 3$ in control; $n = 4$ in ALA, RIF + INH and RIF + INH + ALA groups). * $P < 0.05$ and ** $P < 0.01$ compared with the control group. # $P < 0.05$ compared with RIF + INH group.